

## Conversion of a $\beta$ -strand to an $\alpha$ -helix induced by a single-site mutation observed in the crystal structure of Fis mutant Pro<sup>26</sup>Ala

WEI-ZEN YANG,<sup>1</sup> TZU-PING KO,<sup>1</sup> LEAH CORSELLI,<sup>2</sup> REID C. JOHNSON,<sup>2</sup>  
AND HANNA S. YUAN<sup>1</sup>

<sup>1</sup>Institute of Molecular Biology, Academia Sinica, Taipei, Taiwan 11529, Republic of China

<sup>2</sup>Department of Biological Chemistry, University of California at Los Angeles, Los Angeles, California 90095-1737

(RECEIVED January 13, 1998; ACCEPTED April 6, 1998)

### Abstract

The conversion from an  $\alpha$ -helix to a  $\beta$ -strand has received extensive attention since this structural change may induce many amyloidogenic proteins to self-assemble into fibrils and cause fatal diseases. Here we report the conversion of a peptide segment from a  $\beta$ -strand to an  $\alpha$ -helix by a single-site mutation as observed in the crystal structure of Fis mutant Pro<sup>26</sup>Ala determined at 2.0 Å resolution. Pro<sup>26</sup> in Fis occurs at the point where a flexible extended  $\beta$ -hairpin arm leaves the core structure. Thus it can be classified as a “hinge proline” located at the C-terminal end of the  $\beta$ 2-strand and the N-terminal cap of the A  $\alpha$ -helix. The replacement of Pro<sup>26</sup> to alanine extends the A  $\alpha$ -helix for two additional turns in one of the dimeric subunits; therefore, the structure of the peptide from residues 22 to 26 is converted from a  $\beta$ -strand to an  $\alpha$ -helix. This result confirms the structural importance of the proline residue located at the hinge region and may explain the mutant’s reduced ability to activate Hin-catalyzed DNA inversion. The peptide (residues 20 to 26) in the second monomer subunit presumably retains its  $\beta$ -strand conformation in the crystal; therefore, this peptide shows a “chameleon-like” character since it can adopt either an  $\alpha$ -helix or a  $\beta$ -strand structure in different environments. The structure of Pro<sup>26</sup>Ala provides an additional example where not only the protein sequence, but also non-local interactions determine the secondary structure of proteins.

**Keywords:** conformational change; hinge proline; secondary structural change; X-ray diffraction

The conversion from an  $\alpha$ -helix to a  $\beta$ -strand in proteins, which can lead to the formation of amyloid fibrils and cause diseases, has been investigated by several different biophysical methods (Kelly, 1996). The most widely-known examples are in the prion diseases, such as transmissible bovine spongiform encephalopathy (BSE), or inherited Creutzfeldt-Jacob disease (CJD) (Harrison et al., 1997). It has been shown that inherited prion diseases of humans are all linked to specific point and insertion mutations in the prion protein sequence (Prusiner, 1994). It is believed that the mutations cause part of the prion protein to convert from an  $\alpha$ -helix to a  $\beta$ -strand, which aggregates to form amyloid fibrils in a perpendicular orientation to the long axis of the fibril. Mutations that cause the conversion between coil and  $\alpha$ -helix (Alber et al., 1988) have been reported before, but a change between an  $\alpha$ -helix and a  $\beta$ -strand induced by a single-site mutation has never been directly observed in a three-dimensional structural study. In this study, we show the

conversion from a  $\beta$ -strand to an  $\alpha$ -helix identified in the crystal structure of the Fis mutant Pro<sup>26</sup>Ala.

The 98 amino-acid *Escherichia coli* protein Fis (factor for inversion stimulation) was originally discovered by its ability to regulate DNA inversion catalyzed by the Hin-family of invertases (Johnson et al., 1986; Koch & Kahmann, 1986). In Hin-mediated DNA inversion, Hin invertase dimers bound at the two recombinational sites are responsible for DNA cleavage, exchange, and ligation. Fis activates these catalytic steps by interacting with Hin when bound at two domains within a cis-acting enhancer region (Johnson, 1991). Interactions between Hin and Fis, together with DNA supercoiling, promote the assembly of the invertasome where DNA inversion occurs (Heichman & Johnson, 1990). Fis has also been shown to stimulate  $\lambda$  prophage DNA excision, activate transcription of rRNA and tRNA operons, repress transcription and function in *oriC*-directed DNA replication (Finkel & Johnson, 1992). Other than the need for Fis to bind at specific DNA sites, the mechanisms by which Fis regulates these reactions are different from inversion.

The X-ray crystal structure of wild-type Fis protein has been previously determined and revealed four  $\alpha$ -helices (A to D) from

Reprint requests to: Hanna S. Yang, Institute of Molecular Biology, Academia Sinica, Taipei, Taiwan 11529, Republic of China; e-mail: mbyuan@ccvax.sinica.edu.tw.

residues 27 to 98 (Kostrewa et al., 1991; Yuan et al., 1991). In these orthorhombic crystals, the structure of the N-terminal region prior to residue 27 was not established since electron density for this region was largely absent. The A and B helices from each subunit of the Fis homodimer form a stable helix bundle-like core structure, and the C and D helices are the helix-turn-helix DNA binding motif responsible for direct interactions with DNA. The N-terminal region of Fis, from residues 11 to 36, is functionally important for the stimulation of Hin-mediated inversion, as shown by deletion and single-site mutation studies, and is believed to directly interact with the Hin invertase (Koch et al., 1991; Osuna et al., 1991; Safo et al., 1997). Recently the Fis mutant Lys<sup>36</sup>Glu was crystallized in a different hexagonal form, and its structure revealed that the N-terminal region from residues 10 to 26 contained an extended  $\beta$ -hairpin arm that protruded from the compact core structure (Safo et al., 1997). The  $\beta$ -hairpin arm is constrained at its base where it is connected to the protein core but normally becomes highly mobile as it extends out toward the tip, since there are no surrounding amino acids to stabilize its position. Therefore, the base of the  $\beta$ -hairpin arm (residues 10–13, 24–26) can be observed in the wild-type Fis structure, but the mobile tip region (residues 14–23) has only been seen in the Lys<sup>36</sup>Glu mutant due to interactions with adjacent molecules in the hexagonal crystal. Mutagenesis and cysteine crosslinking studies are entirely consistent with the presence of mobile  $\beta$ -hairpin arms in solution (Safo et al., 1997). Figure 1 shows the structures, the amino acid sequence, and the secondary structure elements of the wild-type and mutant Fis proteins that have been derived from the crystal structures. Based

on extensive mutagenesis, it is believed that the tip of the flexible  $\beta$ -hairpin arm and part of the A-helix interact with Hin to activate recombination.

In the wild-type Fis crystal structure, Pro<sup>26</sup> caps the N-terminal end of the A-helix and the structure is ill-defined prior to this proline. In the Lys<sup>36</sup>Glu mutant, Pro<sup>26</sup> is located at the end of the  $\beta$ -2 strand, which spans residues 22 to 26, and borders onto the A-helix. This paper reports the crystal structure of Fis mutant Pro<sup>26</sup>Ala at 2.0 Å resolution. The replacement of this proline extends the A-helix at the N-terminal end for two additional turns in one of the dimeric subunits. Thus, the structure of the residues 22 to 26 is converted from a  $\beta$ -strand to an  $\alpha$ -helix. This result demonstrates that a single-site mutation at a critical position can induce dramatic secondary structural changes. However, the N-terminal region of the second subunit in the homodimer retains its mobile  $\beta$ -strand conformation, probably due to different packing environments in the crystal. Insights into the details of the  $\beta$ -to- $\alpha$  conformational change, molecular explanations for the reduced activity of the mutant Pro<sup>26</sup>Ala in activating inversion, and factors determining secondary structure are discussed.

## Results

### Overall structure of Pro<sup>26</sup>Ala

The refined structure of Pro<sup>26</sup>Ala highly resembles wild-type Fis as shown in a  $\alpha$ -backbone in Figure 2 in stereo views. In one of

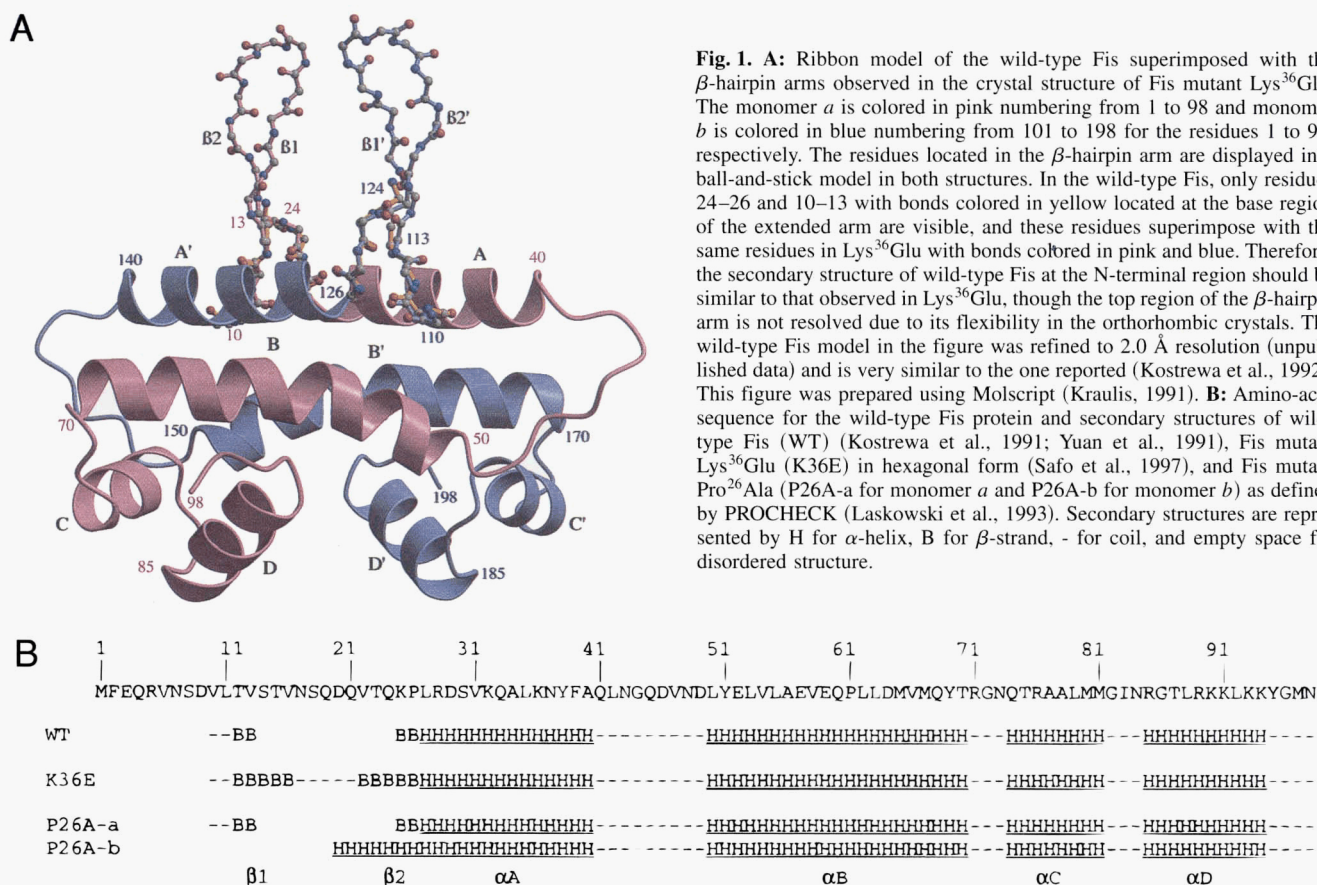


**Fig. 1. A:** Ribbon model of the wild-type Fis superimposed with the  $\beta$ -hairpin arms observed in the crystal structure of Fis mutant Lys<sup>36</sup>Glu. The monomer *a* is colored in pink numbering from 1 to 98 and monomer *b* is colored in blue numbering from 101 to 198 for the residues 1 to 98, respectively. The residues located in the  $\beta$ -hairpin arm are displayed in a ball-and-stick model in both structures. In the wild-type Fis, only residues 24–26 with bonds colored in yellow located at the base region of the extended arm are visible, and these residues superimpose with the same residues in Lys<sup>36</sup>Glu with bonds colored in pink and blue. Therefore, the secondary structure of wild-type Fis at the N-terminal region should be similar to that observed in Lys<sup>36</sup>Glu, though the top region of the  $\beta$ -hairpin arm is not resolved due to its flexibility in the orthorhombic crystals. The wild-type Fis model in the figure was refined to 2.0 Å resolution (unpublished data) and is very similar to the one reported (Kostrewa et al., 1992). This figure was prepared using Molscript (Kraulis, 1991). **B:** Amino-acid sequence for the wild-type Fis protein and secondary structures of wild-type Fis (WT) (Kostrewa et al., 1991; Yuan et al., 1991), Fis mutant Lys<sup>36</sup>Glu (K36E) in hexagonal form (Safo et al., 1997), and Fis mutant Pro<sup>26</sup>Ala (P26A-a for monomer *a* and P26A-b for monomer *b*) as defined by PROCHECK (Laskowski et al., 1993). Secondary structures are represented by H for  $\alpha$ -helix, B for  $\beta$ -strand, - for coil, and empty space for disordered structure.

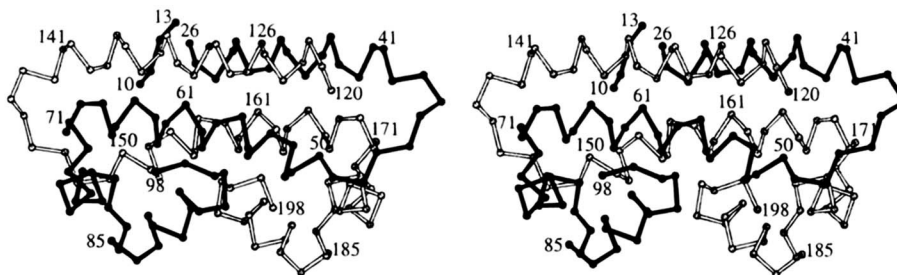


**Fig. 2.** Stereo view of the Fis mutant Pro<sup>26</sup>Ala homodimer represented in a C $\alpha$ -backbone trace with monomer *a* depicted by a heavy line and monomer *b* depicted by a light line. Monomer *a* is modeled from residues 10 to 13 and 26 to 98, and monomer *b* is modeled from 120 to 198. Amino acids 12 to 26 and 112 to 126 normally form  $\beta$ -hairpin structures; however, in Pro<sup>26</sup>Ala, residues 120 to 126 in monomer *b* are converted to an  $\alpha$ -helix structure. Residues 10 to 13 in monomer *a* superimpose with the same residues in Lys<sup>36</sup>Glu or wild-type Fis. This figure was prepared using Molscript (Kraulis, 1991).

the subunits (monomer *a*), like other Fis structures (Kostrewa et al., 1991; Yuan et al., 1991), a fragment of electron density close to the N-terminal region, but discontinuous from the core structure, was present. A tetrapeptide corresponding to Val<sup>10</sup>, Leu<sup>11</sup>, Thr<sup>12</sup>, and Val<sup>13</sup> was assigned to this fragment, consistent with the Lys<sup>36</sup>Glu Fis structure (Safo et al., 1997). Thus, the final model of monomer *a* contains the core structure from residues 26 to 98, and four residues 10 to 13, which are separate from the rest of the molecule. The disorder of the Fis N-terminal region has been a typical problem in earlier studies where wild-type and mutant Fis proteins crystallized in the orthorhombic unit cells (Kostrewa et al., 1991; Yuan et al., 1991, 1994).

However, the other subunit (monomer *b*) in the Pro<sup>26</sup>Ala mutant shows a different secondary structure prior to residue 26. There are six additional residues (120–125) that are clearly visible prior to Ala<sup>126</sup> in monomer *b*, and these residues adopt a completely different secondary structure from that observed in monomer *a* and other wild-type or mutant Fis structures. These residues extend from Ala<sup>126</sup> to form a continuous  $\alpha$ -helix structure resulting in a longer A  $\alpha$ -helix spanning from residues 120–140. Thus, the replacement of proline to alanine extends the A  $\alpha$ -helix by almost two additional turns. In the wild-type Fis, Pro<sup>26</sup> does not contain an amide hydrogen atom, therefore, it cannot make a main-chain hydrogen bond with the -CO group in Val<sup>22</sup>. When the proline is substituted by alanine, the new -NH group is capable of making a hydrogen bond. The bond distance is 2.9 Å between the main-chain nitrogen atom in Ala<sup>26</sup> and the carbonyl oxygen atom in Val<sup>22</sup>.

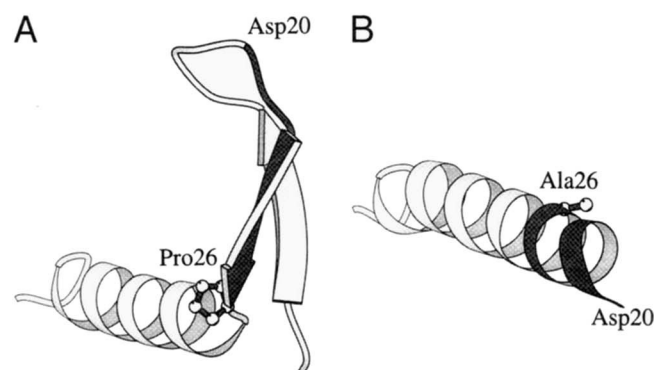
#### Comparison of Pro<sup>26</sup>Ala to wild-type Fis

The core structure of Pro<sup>26</sup>Ala is similar to the wild-type Fis in that it contains the same secondary elements from residues 26 to 98. The least-squares fit of the C $\alpha$ -atoms between wild-type and Pro<sup>26</sup>Ala gives an averaged root-mean-square (RMS) difference of 0.58 Å, slightly higher than what is expected based on the coordinate errors. Almost all of the largest RMS differences between the two structures are concentrated among residues 26–40 (A-helix) and the loop region of 41–46. When only the residues from the B to D helices (residues 50–98) are used for least-squares fitting, the average RMS difference at the C-terminal region is only 0.48 Å, but the average difference between the A-helices is 0.86 Å. The displacement is more pronounced in the A-helix of monomer *b*

(with an RMS difference of 1.05 Å) than that of the monomer *a* (with an RMS difference of 0.63 Å). We found that the A-helix is slightly shifted along the helical axis toward the N-terminal end in the monomer *b*. For comparison, a similar analysis between wild-type Fis and Pro<sup>61</sup>Ala structures gave an RMS difference of only ~0.3 Å that was distributed evenly throughout the entire structure. It has been demonstrated before that Leu<sup>11</sup> is critical for the conformation of the N-terminal region and that a hydrophobic core surrounding Leu<sup>11</sup> interlocks the base of the  $\beta$ -hairpin arm with the core structure of A- and B-helices (Safo et al., 1997). In monomer *b*, Leu<sup>11</sup> is not located at the same position as that of wild-type Fis, and therefore possibly releases the conformational constraint which allows the A-helix to shift.

#### Comparison of Pro<sup>26</sup>Ala to Lys<sup>36</sup>Glu

The comparison between Pro<sup>26</sup>Ala and Lys<sup>36</sup>Glu shows that the most dramatic structural changes are present in the region prior to residue 26 in monomer *b*. A  $\beta$ -strand (residues 22 to 26) and part of the hairpin loop (residues 20 to 21) converted to an  $\alpha$ -helix when an alanine is substituted for Pro<sup>26</sup>. Figure 3 shows the ribbon



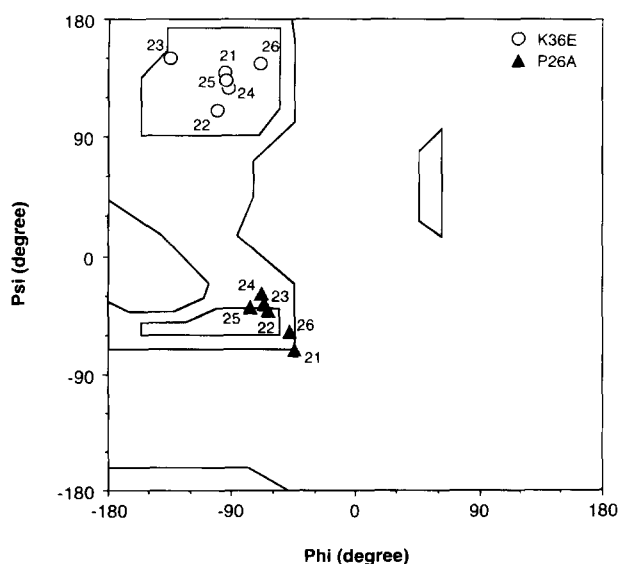
**Fig. 3.** The N-terminal structures of (A) Fis mutant Lys<sup>36</sup>Glu from amino acids 10 to 43, which are believed to exist in wild-type Fis (16), and (B) Pro<sup>26</sup>Ala (monomer *b* amino acids 20 to 43) as displayed in ribbon models. The locations of residues 20 and 26 are labeled in the two structures with the side chains of residues 26 represented in a ball-and-stick model. The regions that converted from a  $\beta$ -strand to an  $\alpha$ -helix after mutation of Pro<sup>26</sup> to alanine are denoted with darker shading.

diagram of Pro<sup>26</sup>Ala and Lys<sup>36</sup>Glu at the N-terminal region, and Figure 4 shows the Ramachandran plot for the residues from 20 to 26 in the two protein structures. It can be clearly seen that the  $\phi$ - $\psi$  angles are clustered at the  $\beta$ -strand region in Lys<sup>36</sup>Glu, but at the  $\alpha$ -helix region in Pro<sup>26</sup>Ala. The  $\phi$ - $\psi$  angles are very similar beyond residue 26 since the secondary structures of Lys<sup>36</sup>Glu and Pro<sup>26</sup>Ala are identical from residues 26 to 98. The  $\phi$ - $\psi$  angles in Pro<sup>26</sup>Ala start to change right at position 26 due to the mutation. Thus, an amino acid substitution of a proline that caps the N-terminal end of an  $\alpha$ -helix extends the helix for two additional turns. A related phenomenon has been reported before in a phage T4 lysozyme mutant structure in which a loop was converted into an  $\alpha$ -helix by substituting a proline at the N-terminal end of an  $\alpha$ -helix with seven different residues (Alber et al., 1988).

In monomer *a*, residues 10–13 and 25–26 of Pro<sup>26</sup>Ala are located at the same place as the corresponding ones in Lys<sup>36</sup>Glu. This implies that the N-terminal region of monomer *a* retains the structure of the  $\beta$ -hairpin arm, but the tip of the arm is disordered due to its mobility in the orthorhombic unit cell. Thus, we can only observe part of the structure at the base of the flexible arm in this region. The structure of the mobile  $\beta$ -hairpin arm in Fis has been described and discussed earlier (Safo et al., 1997). The different secondary structures generated from the same amino acid sequence in monomers *a* and *b* may be due to different packing environments, which will be addressed in Discussion.

#### CD studies of Fis mutant Pro<sup>26</sup>Ala

CD spectra have been recorded for both wild-type Fis and Pro<sup>26</sup>Ala mutant proteins under the same conditions. The estimated percentages for the secondary structural elements are 80.4%  $\alpha$ -helix and 9.2%  $\beta$ -sheet for wild-type Fis, and 80.3%  $\alpha$ -helix and 8.5%  $\beta$ -sheet for Pro<sup>26</sup>Ala as calculated by the program Selcon (Sreerama & Woody, 1993). The percentage of  $\beta$ -sheets does decrease for the



**Fig. 4.** Ramachandran plot for residues 20 to 26 (monomer *b*) in Fis mutant Pro<sup>26</sup>Ala (represented by  $\blacktriangle$ ) and Lys<sup>36</sup>Glu (represented by  $\circ$ ). The Phi-Psi angles are clustered in the  $\alpha$ -helix region in Pro<sup>26</sup>Ala, but in the  $\beta$ -strand region in Lys<sup>36</sup>Glu.

Pro<sup>26</sup>Ala mutant, but the difference is small. Therefore, the structure of Pro<sup>26</sup>Ala in solution should be similar to the wild-type Fis, consistent with the crystal structure studies.

#### Structural differences in solution resulting from the Pro<sup>26</sup>Ala mutation as measured by the formation of an intersubunit disulfide bond

Rates of disulfide bond formation between cysteines located within the N-termini of the Fis dimer subunits were measured to provide biochemical evidence for a structural difference in this region caused by the Pro<sup>26</sup>Ala mutation. The comparison of oxidation rates between cysteines substituted at different positions within the N-terminus has provided strong support for the  $\beta$ -hairpin arm structure in solution that is observed by crystallography (Safo et al., 1997). One of the substitutions that most efficiently oxidized into a disulfide linkage was Ser<sup>18</sup>Cys. Serine 18 is located near the top of the  $\beta$ -hairpin loop, and the side chains from each subunit at this position are oriented appropriately to readily associate, given the predicted flexibility of the  $\beta$ -arms. Thus, rates of disulfide formation between subunits in the Ser<sup>18</sup>Cys dimer can be used as a solution probe of the  $\beta$ -hairpin arm structure. Pro<sup>26</sup>Ala was combined with Ser<sup>18</sup>Cys and disulfide formation rates of the double mutant were compared with Ser<sup>18</sup>Cys. The purified proteins were initially reduced with dithiothreitol, followed by dialysis to remove the DTT, and then subjected to oxidation in the presence of 1 mM oxidized glutathione. The percent of disulfide-linked protein at various time points was determined by non-reducing SDS-PAGE followed by densitometry. As shown in Figure 5, disulfide bond

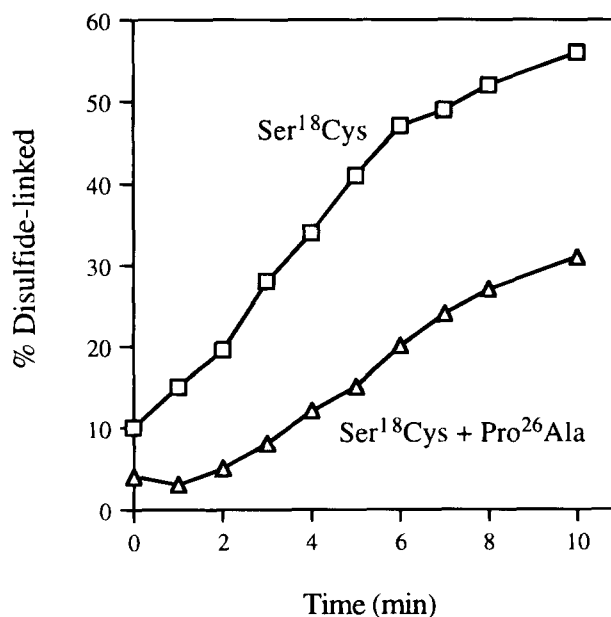


**Fig. 5.** Rates of intersubunit disulfide formation within Ser<sup>18</sup>Cys and Pro<sup>26</sup>Ala + Ser<sup>18</sup>Cys dimers. Reduced preparations of Ser<sup>18</sup>Cys and Pro<sup>26</sup>Ala + Ser<sup>18</sup>Cys were exposed to 1 mM oxidized glutathione at a concentration of 2  $\mu$ M at 23  $^{\circ}$ C as described (Safo et al., 1997). Aliquots were removed at various times, quenched in SDS sample buffer, and electrophoresed in a non-reducing SDS-PAGE gel. The percent of disulfide-linked dimers at each time point is given.

formation in the presence of Pro<sup>26</sup>Ala occurs relatively efficiently, but the rate is about 50% that of Ser<sup>18</sup>Cys. This result provides evidence that the normal  $\beta$ -hairpin structure is partially, but not completely, disrupted by Pro<sup>26</sup>Ala in solution. Similar oxidation experiments have also been performed in various concentrations of trifluoroethanol (TFE), which is known to enhance helix formation in model peptides (Jasanoff & Fersht, 1994; Luo & Baldwin, 1997). The presence of 1–10% TFE greatly decreased disulfide bond formation within Pro<sup>26</sup>Ala + Ser<sup>18</sup>Cys dimers but only had a small effect on Ser<sup>18</sup>Cys (data not shown). Higher amounts of TFE inhibited disulfide formation in both mutants, suggesting that the  $\beta$ -arm structure is disrupted under these conditions even without the Pro<sup>26</sup>Ala substitution. These data imply that the N-terminal region of the Pro<sup>26</sup>Ala subunits may be in an equilibrium between the  $\alpha$ -helical and the normal  $\beta$ -strand structures under standard aqueous solution conditions, and that relatively small changes in environmental conditions can shift the equilibrium into predominantly the helical form.

#### Activities of Fis mutant Pro<sup>26</sup>Ala

The N-terminal  $\beta$ -hairpin arm region of Fis mediates activation of Hin-catalyzed DNA inversion, though only one  $\beta$ -arm within the Fis dimer is sufficient. Figure 6 shows the functional consequences of the Pro<sup>26</sup>Ala substitution on the ability of Fis to stimulate Hin inversion in vitro. The rate of Hin-catalyzed DNA inversion in the presence of Pro<sup>26</sup>Ala is about 40% of that measured for the wild type protein, consistent with a portion of the Fis dimers containing a disrupted  $\beta$ -arm region. A qualitatively similar decrease in its inversion activation activity is also observed in vivo (data not shown). The reduced form of the Pro<sup>26</sup>Ala + Ser<sup>18</sup>Cys double mutant also showed a 60% decrease in Hin inversion activation as

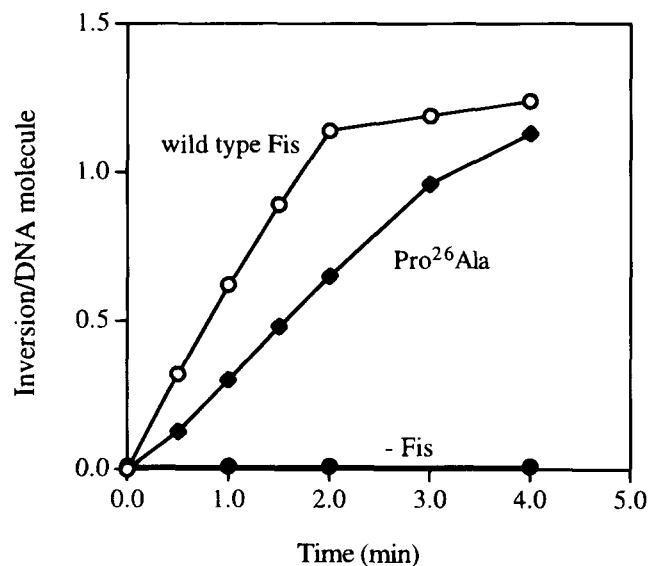


**Fig. 6.** In vitro activation of Hin-mediated DNA inversion by Fis mutant Pro<sup>26</sup>Ala. Reaction solutions contained 40 nM wild-type (WT) or Pro<sup>26</sup>Ala (P26A) Fis, 50 nM Hin, 200 nM HU, and 4 nM supercoiled pMS551 DNA. Aliquots were taken at different times and the number of inversions per DNA substrate molecule was determined after restriction digestion and gel electrophoresis as described (Johnson et al., 1986).

compared with Ser<sup>18</sup>Cys, which gives wild-type activity whether it is reduced or disulfide-linked (Safo et al., 1997). When Pro<sup>26</sup>Ala + Ser<sup>18</sup>Cys was disulfide-linked, however, its activity was found to be indistinguishable from wild type. This result is predicted since the disulfide linkage would fix the N-termini of both subunits of the double mutant in the active  $\beta$ -hairpin arm configuration. In fact, a 2.5 Å electron density map of orthorhombic crystals of oxidized Pro<sup>26</sup>Ala + Ser<sup>18</sup>Cys reveals that both subunits have adopted the  $\beta$ -hairpin arm structure at their N-termini (data not shown).

Pro<sup>26</sup>Ala was also quantitatively assayed for its ability to stimulate phage  $\lambda$  excision in vivo (Ball & Johnson, 1991), activate *proP* transcription in vivo (Xu & Johnson, 1995), and bind and bend DNA in vitro by a gel mobility shift assay (Wu & Crothers, 1984). As expected, none of these activities were significantly altered (Table 1), since they are each mediated by residues within the C-terminal end of the protein where there are no observable differences in the crystal structure. Thus, the functional properties of the protein are entirely consistent with its crystal structure.

#### Discussion

Proline differs from other amino acids in that it does not contain the amide hydrogen atom and its side chain is covalently bonded to the preceding peptide bond nitrogen which introduces local rigidity to the peptide chain. Therefore, the proline residue is often located at the first position (N1 position) of an  $\alpha$ -helix, which is believed to be primarily due to its highly restricted backbone conformation that is energetically favorable in forming a regular structure (Richardson & Richardson, 1988). Proline is also classified as an unfavorable N-capping residue, mostly because its side chain cannot interact with the N-terminus of the helix (Doig & Baldwin, 1995; Doig et al., 1997). Moreover, it has been noted that protein-protein contacts are increased in a number of protein oligomers by an arm exchange or a domain swapping process, and proline residues frequently occur at the base of exchanged arms (Bergdoll et al., 1997). In this context, they are described as "hinge prolines," and the occurrence of proline at a hinge region is explained by the

**Table 1.** Activities of wild-type Fis and mutant Pro<sup>26</sup>Ala

Mutant	Inversion <sup>a</sup>	$\lambda$ excision <sup>b</sup>	Transcription <sup>c</sup>	DNA binding <sup>d</sup>
Wild type	0.60	275	150	$2 \times 10^{-9}$
- Fis	<0.01	1	1	
Pro <sup>26</sup> Ala	0.24	255	138	$2 \times 10^{-9}$

<sup>a</sup>Rates of Fis-activated Hin catalyzed DNA inversions in vitro using purified proteins (Johnson et al., 1986). Values represent inversions per DNA substrate molecule per minute.

<sup>b</sup>Fold stimulation of phage  $\lambda$  excision by Fis in vivo (Ball & Johnson, 1991). Values are given relative to the no Fis, control which gave  $6 \times 10^7$  plaque forming units per mL.

<sup>c</sup>Fis-activation of *proP* P2 transcription in vivo (Xu & Johnson, 1995). Values are given relative to the no Fis control, which gave 4.5 units of  $\beta$ -galactosidase activity programmed from a *proP-lacZ* fusion.

<sup>d</sup> $K_d$  (M) as determined by gel mobility shift assays using the *hin* enhancer distal Fis binding site as a probe (Pan et al., 1996). The wild-type and Pro<sup>26</sup>Ala DNA complexes migrated identically when the binding site was located near the middle of the DNA fragment, indicating that Fis-induced DNA bending was the same.

rigidity of the proline residue and the extended conformation of the peptide chain that is favored by prolines.

Pro<sup>26</sup> in Fis occurs at the point where the  $\beta$ -hairpin arm leaves the core structure, thus it can be classified as a "hinge proline" located at the end of a  $\beta$ -strand in a trans-conformation and N-capping the A-helix. Pro<sup>26</sup>, therefore, should be very important in orienting the conformation of the  $\beta$ -hairpin arm. We find that replacing this proline with an alanine results in extending the A  $\alpha$ -helix for two additional turns at its N-terminal end in one of the Fis monomer subunits. This structural change can be explained in several ways. First, although the helix propensities for the neighboring residues (<sup>20</sup>DQVTQK<sup>25</sup>) are generally low, the Pro<sup>26</sup>Ala mutation substitutes the least favored amino acid for the most favored amino acid in an  $\alpha$ -helix, thereby increasing the helix propensity substantially (O'Neill & DeGrado, 1990; Blaber et al., 1993). The Fis mutant Pro<sup>26</sup>Leu has also been crystallized in the same orthorhombic unit cell, but the electron density prior to Leu<sup>26</sup> is not as well defined as observed for Pro<sup>26</sup>Ala. Only broken density in the shape of a helix is obtained in subunit *b* (data not shown). This difference may reflect the lower helix propensity for leucine as compared with alanine, resulting in Pro<sup>26</sup>Leu forming a less stable extended helix. Second, it has been shown before that the tertiary context is a major determinant of  $\beta$ -sheet propensity while the intrinsic ability for an amino acid to form a  $\beta$ -strand structure only contributes a minor role (Minor & Kim, 1994). The peptide of <sup>20</sup>DQVTQKA<sup>26</sup> is located at the edge of the Fis molecule and is highly exposed to solvent; therefore, the tertiary context influence to direct a  $\beta$ -sheet structure is reduced. Third, this peptide does not contain strong periodicity of polar and nonpolar amino acids of 3.6 residues for  $\alpha$ -helices or 2 residues for  $\beta$ -sheets (Xiong et al., 1995). The combination of the second and third factors should result in a peptide that is more flexible and more capable of adopting different secondary structures.

The conversion from an  $\alpha$ -helix to a  $\beta$ -strand has attracted extensive attention since it is believed that this type of structural change induces many amyloidogenic proteins to self-assemble into fibrils and cause fatal diseases. Thus it is important to know what types of mutations can induce such a structural rearrangement, which may help in the development of rational approaches to the treatment of amyloid diseases. The recently solved NMR structure of the mouse prion protein PrP domain (amino acids 121–231) shows that most of the mutations associated with inherited prion diseases are located in regular secondary structural elements or immediately adjacent to them (Riek et al., 1996). The structure of Pro<sup>26</sup>Ala indeed confirms that a single-site mutation can induce dramatic structural changes, especially if the mutation occurs at the junction of different secondary structures.

While the residues from 22 to 26 convert from a  $\beta$ -strand to an  $\alpha$ -helix in subunit *b* in the Fis homodimer, the same region from subunit *a* presumably retains the  $\beta$ -strand structure. Therefore, even though the protein sequence is the same, the two peptide fragments with the sequence of <sup>20</sup>DQVTQKA<sup>26</sup> have different secondary structures in the Pro<sup>26</sup>Ala mutant. Because there are two molecules per asymmetric unit in the orthorhombic unit cell, the two Fis subunits are not crystallographically identical and have different crystal packing environments. It has been shown before that non-local interactions of amino acids from the tertiary structure of a protein can be an important factor in determining the secondary structure of peptides (Waterhous & Johnson, 1994). The report of a "chameleon" sequence of 11 residues that folds as an  $\alpha$ -helix or a  $\beta$ -strand when inserted in different positions in the

immunoglobulin-binding domain of protein G also demonstrates the importance of the non-local interactions in determining the secondary structure (Minor & Kim, 1996). Thus, the structure of Fis mutant Pro<sup>26</sup>Ala provides another example where the same peptide sequence can form different secondary structures when exposed to different environments. An  $\alpha$  to  $\beta$  conformational switch has also been observed before in structures of the elongation factor EF-Tu in which a peptide fragment of six amino acids in length within a  $\beta$ -hairpin, converts from a  $\beta$ -strand in the GDP form to an  $\alpha$ -helix in the GTP complex (Abel et al., 1996). In addition, the report of the crystal structure of the yeast MAT $\alpha$ 2/MCM1/DNA ternary complex (Tan & Richmond, 1998) shows that the originally flexible amino-terminal extension of the MAT $\alpha$ 2 homeo-domain forms a  $\beta$ -hairpin when it interacts with MCM1. Within this  $\beta$ -hairpin, an eight-amino-acid sequence adopts a  $\beta$ -strand conformation in one of the dimeric subunit, but changes to an  $\alpha$ -helical conformation in the other subunit. Interestingly, the  $\beta$ -hairpin arm in Fis is also responsible for direct interactions with Hin invertase. It seems that protruding  $\beta$ -hairpins can display extensive polymorphism, particularly when they bind other proteins or substrates.

The alternative secondary structures observed in the Pro<sup>26</sup>Ala crystal structure are probably present in solution where different microsolvant environments would influence their interconversion. Under standard aqueous solution conditions, there is a moderately slower rate of disulfide formation between Cys<sup>18</sup> residues in the dimer when the Pro<sup>26</sup>Ala mutation is present. This effect is strongly enhanced when small amounts of trifluoroethanol are added, implying that the equilibrium is shifted such that the  $\alpha$ -helical conformer now predominates over the  $\beta$ -hairpin. The reduced ability of Pro<sup>26</sup>Ala to activate Hin inversion, both in vitro and in vivo, is also fully consistent with the structural changes seen in the crystal. Recent experiments suggest that amino acids in only one arm of each Fis dimer are minimally required for activation of the Hin invertasome (S. Merickel & R.C. Johnson, unpubl. data). Thus, only one structurally intact  $\beta$ -hairpin arm in Pro<sup>26</sup>Ala would be sufficient to allow Fis to productively interact with the Hin recombinase.

## Materials and methods

### Construction and purification of Fis mutant proteins

The Pro<sup>26</sup>Ala mutation (CCC to GCC) was introduced into pRJ807 (Osuna et al., 1991) by the two-step polymerase chain reaction method (Landt et al., 1990) to generate pRJ1136. For large-scale overproduction, the mutant gene was transferred into pET11a (Novagen, USA) and transformed into RJ1852 (BL21 fis-767) (Pan et al., 1996). The mutant Fis protein was purified to >98% homogeneity by chromatography on S-Sepharose (Pharmacia, Sweden) followed by an FPLC mono-S column (Pan et al., 1996). After dialysis against a low-salt buffer (0.05 M NaCl and 20 mM Tris-HCl, pH 8.2), the precipitated Fis was resolubilized and stored at a concentration of 30 mg/mL in 20 mM Tris-HCl (pH 8.2), 1.0 M NaCl at  $-70^{\circ}\text{C}$ . Mass spectroscopy measured a molecular mass of 11,216( $\pm$ 3) for Pro<sup>26</sup>Ala, compared with 11,213 calculated from the predicted amino-acid sequence.

The Ser<sup>18</sup>Cys mutation (TCT to TGT) was combined with Pro<sup>26</sup>Ala by performing a PCR reaction using pRJ1136 as a template and a 5' oligonucleotide primer that overlapped the unique *Hpa*I site in the *fis* gene and contained the Ser<sup>18</sup>Cys mutation. The

product was cleaved with *Hpa*I and *Hind*III, which is located beyond the 3' end of the *fis* gene and used to replace the analogous fragment in pRJ1077 (pET11a-*fis* wild-type) (Pan et al., 1996).

#### Measurement of circular dichroism spectra

The circular dichroism (CD) spectra were measured with the wavelength varying from 180 to 260 nm on a Jasco J-700 spectropolarimeter. The protein concentration was adjusted to 0.02 mg/mL in a buffer solution of 10 mM potassium phosphate at pH 7.5. The percentage of the secondary structure was calculated by the program Selcon (Sreerama & Woody, 1993).

#### Crystallization and data collection

Crystals of Pro<sup>26</sup>Ala were grown by the hanging drop vapor diffusion method from a solution of 15 mg/mL protein, 0.5 M NaCl, 10 mM Tris-HCl (pH 8.2), and 10% PEG4000, against a reservoir of 20% PEG4000. Large rectangular crystals (approximately 0.3 × 0.4 × 0.8 mm<sup>3</sup>) were obtained after several days at room temperature.

The diffraction data were recorded at room temperature by an R-AXIS II imaging plate equipped with a rotating anode and a double-mirror focusing system. The crystals were isomorphous to the previously solved wild-type Fis (Yuan et al., 1991) and mutant Pro<sup>61</sup>Ala (Yuan et al., 1994) with orthorhombic P2<sub>1</sub>2<sub>1</sub>2<sub>1</sub> unit cells. The crystallographic details are listed in Table 2. A total of 64,153 reflections were recorded and reduced to 13,188 unique reflections with an  $R_{sym}$  of 7.4% based on the intensities between symmetry-related reflections. The merged data set corresponds to 94.6% of the possible data up to 2.0 Å resolution.

#### Refinement

The previously determined isomorphous Fis mutant protein structure Pro<sup>61</sup>Ala (Yuan et al., 1994) was used as a starting model for the Pro<sup>26</sup>Ala refinement. There are two monomers, *a* and *b*, per asymmetric unit, and their residues are numbered from 1 to 98 and 101 to 198 in each monomer, respectively. The model of Pro<sup>61</sup>Ala contains residues 26 to 98 in two subunits and two discontinuous tetra-peptide fragments (residues 10 to 13 and 110 to 113) located at the N-terminal region. Only the model comprising the continuous polypeptide chains of 26–98 amino acid residues of the two monomers were used, and Pro<sup>26</sup> was changed to alanine and Ala<sup>61</sup> was changed to proline prior to refinement. The model was subjected to a rigid body refinement to a crystallographic *R*-factor of 38.7% using data between 8.0–2.5 Å with the two monomers treated as two independent groups. A series of positional and simulated annealing refinements to a resolution of 2.0 Å were gradually undertaken. A continuous stretch of density from the Ala<sup>126</sup> of monomer *b* was observed, and six residues were added to this density to form a continuous polypeptide chain of 120–198 amino acids. The omitted electron density map at the N-terminal end of monomer *b* is shown in Figure 7A. A continuous helix-shaped density can be clearly observed prior to residue 27, and this density disappeared at residue 20. The side chains of Asp<sup>20</sup>, Val<sup>22</sup>, Thr<sup>23</sup>, and Gln<sup>24</sup> are well defined in the final ( $2F_o - F_c$ ) map (Fig. 7B), but the side chains of Gln<sup>21</sup> and Lys<sup>25</sup> are broken. On the other hand, in monomer *a*, a stretch of density close to, but separated

**Table 2.** X-ray diffraction statistics for the Fis mutant Pro<sup>26</sup>Ala

Data collection and processing	
Space group	P2 <sub>1</sub> 2 <sub>1</sub> 2 <sub>1</sub>
Cell dimensions (Å)	
<i>a</i> =	80.62
<i>b</i> =	51.11
<i>c</i> =	47.85
Resolution (Å)	2.00
Observed reflections	64,153
Unique reflections	13,188
Completeness—all data (%)	94.6
$R_{merge}$ —all data <sup>a</sup>	7.4
Refinement	
Resolution range (Å)	8.0–2.00 ( $F > 2\sigma F$ )
Reflections	11,745
Non-hydrogen atoms	
Protein	1,249
Solvent molecules	103
<i>R</i> -factor (%)	20.2
<i>R</i> -free (%)	28.0
Model quality	
RMS deviations in	
Bond lengths (Å)	0.010
Bond angles (°)	1.187
Average <i>B</i> -factor (Å <sup>2</sup> )	
Non-hydrogen atoms	33.1
Protein atoms	32.4
Solvent atoms	41.2

$$^a R_{merge} = \frac{\sum_h \sum_i |I_{h,i} - \langle I_h \rangle|}{\sum_h \sum_i I_{h,i}}, \text{ where } \langle I_h \rangle \text{ is the mean intensity of the}$$

*i* observations for a given reflection *h*.

from, the N-terminal region was observed. This stretch of density corresponded to a discontinuous region observed in wild-type and Pro<sup>61</sup>Ala Fis crystals and was fitted with the residues Val<sup>10</sup>, Leu<sup>11</sup>, Thr<sup>12</sup>, and Val<sup>13</sup> (Safo et al., 1997). At this stage 8% of the total reflection data were excluded from the refinement and used to calculate the *R*-free. The model was then taken through several cycles of alternate positional and simulated annealing. Addition of 103 waters (*B*-factors less than 60 Å<sup>2</sup>) and *B*-factor refinement resulted in a final *R*-factor of 20.2% and *R*-free of 28.0% based on 11,745 reflections ( $F > 2\sigma F$ ) in the resolution range of 8.0–2.0 Å.

The final model of Pro<sup>26</sup>Ala consisted of 1,249 protein atoms and 103 water molecules. Residues 1–9 and 14–25 of monomer *a* were not included in the model due to the absence of any interpretable electron density. Likewise, residues 101–119 of monomer *b* were not included. Overall the model has acceptable stereochemistry, with RMS deviations of bond lengths and bond angles of 0.010 Å and 1.187°, respectively. A PROCHECK analyses of the Ramachandran plot of the main-chain conformational angles show that 90.6% lie in the core region with 8.8% residing in the allowed region. One residue, Asn<sup>43</sup>, lies in the disallowed region. This residue is located in a loop region and has poor electron density. There is a break in the main-chain electron density at Asn<sup>43</sup> and Asn<sup>84</sup>. Six other residues, Gln<sup>121</sup>, Lys<sup>136</sup>, Gln<sup>141</sup>, Asn<sup>143</sup>, Gln<sup>145</sup>, and Asn<sup>198</sup>, show poor densities of their side chains.

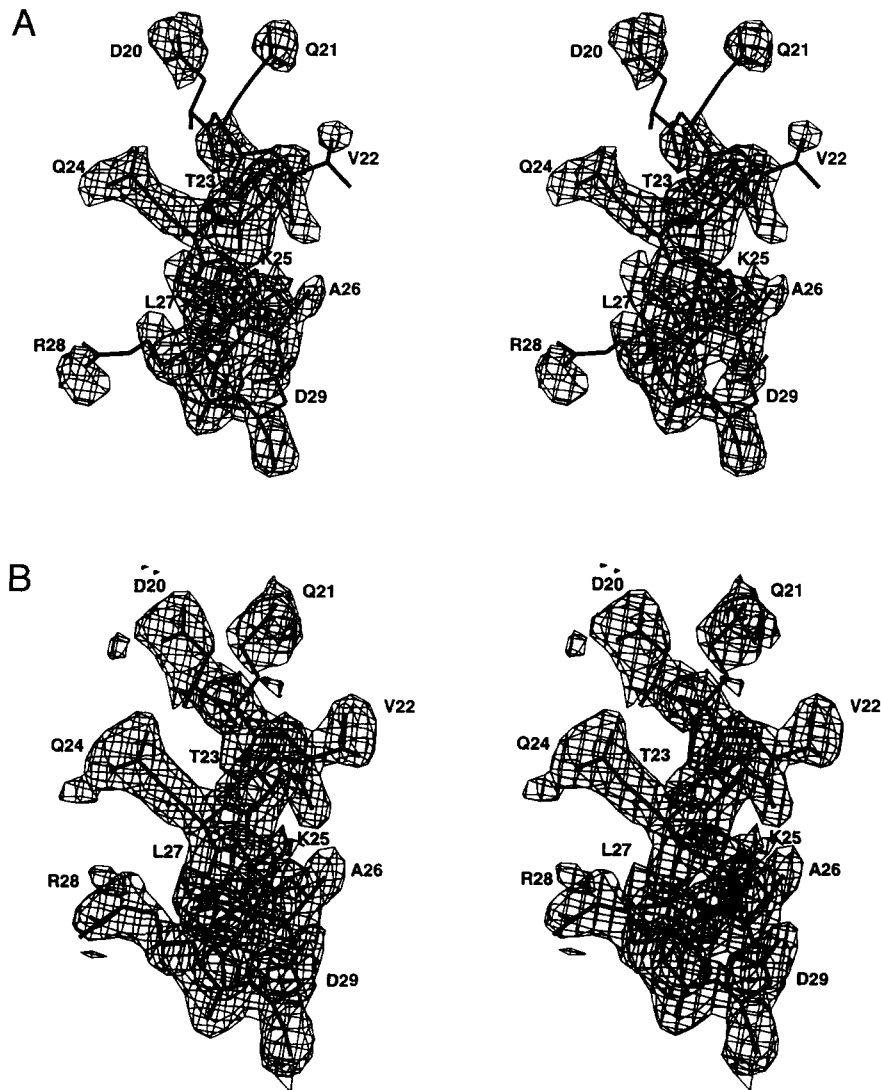


**Fig. 7. A:** Stereo view of the omit ( $2F_o - F_c$ ) electron-density map for Fis Pro<sup>26</sup>Ala at the N-terminal region of monomer *b*. The density extends in a helix configuration from residues 20 to 26, unlike that observed in monomer *a* of Fis Pro<sup>26</sup>Ala or either subunit of wild-type Fis. The map was calculated by omitting residues 20 to 26 in monomer *b* of the Fis homodimer. Simulated annealing refinement was done with a 3 Å spherical shell of fixed atoms surrounding the omitted regions, and the maps were contoured at  $0.8\sigma$  of the average electron density. **B:** Stereo view of the final ( $2F_o - F_c$ ) map calculated with  $\alpha_{cat}$ . The map is contoured at the  $1\sigma$  level.

### Acknowledgments

We thank S. Finkel and S. Cramton for providing data, and Ming F. Tam for determining the molecular mass of proteins by mass spectroscopy. This work was supported by research grants from the Academia Sinica and the National Science Council (NSC87-2311-B001-072) of Republic of China in Taiwan to Hanna S.Yuan, and by the National Institutes of Health (GM38509) to Reic C. Johnson.

### References

- Abel K, Yoder MD, Higenfeld R, Jurnak F. 1996. An  $\alpha$  to  $\beta$  conformational switch in EF-Tu. *Structure* 4:1153–1159.
- Alber T, Bell JA, Sun D-P, Nicholson H, Wozniak JA, Cook S, Matthews BW. 1988. Replacement of Pro-86 in phage T4 lysozyme extend an alpha-helix but do not alter protein stability. *Science* 239:631–635.
- Ball BA, Johnson RC. 1991. Efficient excision of phage lambda from the *Escherichia coli* chromosome requires the Fis protein. *J Bacteriol* 173:4027–4031.
- Bergdoll M, Remy M-H, Cagnon C, Masson J-M, Dumas P. 1997. Proline-dependent oligomerization with arm exchange. *Structure* 5:391–401.
- Blaber M, Zhang X-J, Matthews BW. 1993. Structural basis of amino acid  $\alpha$  helix propensity. *Science* 260:1637–1640.
- Doig AJ, Baldwin RL. 1995. N- and C-capping preferences for all 20 amino acids in  $\alpha$ -helical peptide. *Protein Sci* 4:1325–1336.
- Doig AJ, MacArthur MW, Stapley BJ, Thornton JM. 1997. Structure of N-termini of helices in proteins. *Protein Sci* 6:147–155.
- Finkel SE, Johnson RC. 1992. The Fis protein: It's not just for DNA inversion anymore. *Mol Microbiol* 6:3257–3265.
- Harrison PM, Bamborough P, Daggett V, Prusiner SB, Cohen FE. 1997. The prion folding problem. *Curr Opin Struct Biol* 7:53–59.
- Heichman KA, Johnson RC. 1990. The Hin invertasome: Protein-mediated joining of distant recombination sites at the enhancer. *Science* 249:511–517.
- Jasanoff A, Fersht AR. 1994. Quantitative determination of helical propensities from trifluoroethanol titration curves. *Biochemistry* 33:2129–2135.
- Johnson R. 1991. Mechanism of site-specific DNA inversion in bacteria. *Curr Opin Gen Devel* 1:404–411.
- Johnson RC, Bruist MF, Simon MI. 1986. Host protein requirements for in vitro site-specific DNA inversion. *Cell* 46:531–539.



- Kelly JW. 1996. Alternative conformations of amyloidogenic proteins govern their behavior. *Curr Opin Struct Biol* 6:11–17.
- Koch C, Kahmann R. 1986. Purification and properties of the *Escherichia coli* host factor required for inversion of the G segment in bacteriophage Mu. *J Biol Chem* 261:15673–15678.
- Koch C, Ninnemann O, Fuss H, Kahmann R. 1991. The N-terminal part of the *E. coli* DNA binding protein Fis is essential for stimulating site-specific DNA inversion but is not required for specific DNA binding. *Nucleic Acids Res* 19:5915–5922.
- Kostrewa D, Granzin J, Koch C, Choe H-W, Raghunathan S, Wolf W, Kahmann R, Saenger W. 1991. Three-dimensional structure of the *E. coli* DNA-binding protein Fis. *Nature* 349:178–180.
- Kostrewa D, Granzin J, Stock D, Choe H-C, Labahn J, Saenger W. 1992. Crystal structure of the Factor for Inversion Stimulation FIS at 2.0 Å resolution. *J Mol Biol* 226:209–226.
- Kraulis PJ. 1991. MOLSCRIPT: A program to produce both detailed and schematic plots of protein structures. *J Appl Cryst* 24:946–950.
- Landt O, Grunert H, Hahn U. 1990. A general method for rapid site-directed mutagenesis using the polymerase chain reaction. *Gene* 96:125–128.
- Laskowski RA, MacArthur MW, Moss DS, Thornton JM. 1993. PROCHECK: A program to check the stereochemical quality of protein structures. *J Appl Cryst* 26:283–291.
- Luo P, Baldwin RL. 1997. Mechanism of helix induction by trifluoroethanol: A framework for extrapolating the helix-forming properties of peptides from trifluoroethanol/water mixtures back to water. *Biochemistry* 38:8413–8421.
- Minor DL, Kim PS. 1994. Context is a major determinant of  $\beta$ -sheet propensity. *Nature* 371:264–267.
- Minor DL, Kim PS. 1996. Context-dependent secondary structure formation of a designed protein sequence. *Nature* 380:730–734.
- O'Neill KT, DeGrado WF. 1990. A thermodynamic scale for the helix-forming tendencies of the commonly occurring amino acids. *Science* 250:646–651.
- Osuna R, Finkel SE, Johnson RC. 1991. Identification of two functional regions in Fis: The N-terminus is required to promote Hin-mediated DNA inversion but not lambda excision. *EMBO J* 10:1593–1603.
- Pan, CQ, Finkel SE, Cramton SE, Sigman DS, Johnson RC. 1996. Variable structures of Fis-DNA complexes determined by flanking DNA contacts. *J Mol Biol* 264:675–695.
- Prusiner SB. 1994. Molecular biology and genetics of prion disease. *Phil Trans R Soc Lond B* 343:447–463.
- Richardson JS, Richardson DC. 1988. Amino acid preferences for specific locations at the ends of  $\alpha$  helix. *Science* 240:1648–1652.
- Riek R, Hornemann S, Wider G, Billeter M, Glockshuber R, Wuthrich K. 1996. NMR structure of the mouse prion protein domain PrP (121–231). *Nature* 382:180–182.
- Safo MK, Yang WZ, Corselli L, Cramton SE, Yuan HS, Johnson RC. 1997. The transactivation region of the Fis protein that controls site-specific DNA inversion contains extended mobile  $\beta$ -hairpin arms. *EMBO J* 16:6860–6873.
- Sreerama N, Woody RW. 1993. A self-consistent method for the analysis of protein secondary structure from circular dichroism. *Anal Biochem* 209:32.
- Tan S, Richmond TJ. 1998. Crystal structure of the yeast MAT $\alpha$ 2/MCM1/DNA ternary complex. *Nature* 391:660–666.
- Waterhous VD, Johnson CW. 1994. Importance of environment in determining secondary structure in proteins. *Biochemistry* 33:2121–2128.
- Wu HM, Crothers DM. 1984. The locus of sequence-directed and protein-induced DNA bending. *Nature* 308:509–513.
- Xiong H, Buckwalter BL, Shieh H-M, Kecht MH. 1995. Periodicity of polar and nonpolar amino acids is the major determinant of secondary structure in self-assembling oligomeric peptides. *Proc Natl Acad Sci USA* 92:6349–6353.
- Xu J, Johnson RC. 1995. *aldB*, an RpoS-dependent gene in *Escherichia coli* encoding an aldehyde dehydrogenase that is repressed by Fis and activated by Crp. *J Bacteriol* 177:3166–3175.
- Yuan HS, Wang SS, Yang W-Z, Finkel SE, Johnson RC. 1994. The structure of Fis mutant Pro61-Ala illustrates that the kink within the long alpha-helix is not due to the presence of the proline residue. *J Biol Chem* 269:28947–28954.
- Yuan SH, Finkel SE, Feng JA, Kaczor-Grezskowiak M, Johnson RC, Dickerson RE. 1991. The molecular structure of wild-type and a mutant Fis: Relationship between mutational changes and recombinational enhancer function or DNA bending. *Proc Natl Acad Sci USA* 88:9558–9562.